19th Brazilian Congress of Thermal Sciences and Engineering
November 06th-10th, 2022, Bento Gonçalves - RS - Brazil

ENC-2022-0661
PERFORMANCE ANALYSIS OF DOUBLE CASCADE HEAT PUMP FOR INDUSTRIAL STEAM GENERATION

Lorena Barros Guimarães
Emmanuel Damilano Dutra
Universidade Federal de Pernambuco, Cidade Universitária, Recife - PE, 50740-540.
lorena.bguimaraes@ufpe.br
emmanuel.dutra@ufpe.br

Luis Arturo Gómez-Malagón
Universidade de Pernambuco, R. Benfica, 455 - Madalena, Recife - PE, 50720-001.
lagomezma@poli.br

Abstract. *Conventionally, industrial steam production comes from wood-fired or Liquefied Petroleum Gas (LPG) boilers. However, to reduce CO_2 emissions in heat generation process, double cascade heat pumps (DCHP) point to an opportunity for decarbonization and improvement of operational and economic performance. Therefore, this work aims to perform the thermal modeling of a DCHP to generate steam and water cooling for an industrial process. Moreover, the comparative global warming potential (GWP) between the proposed system and the conventional technologies was also determined. The effect of the condensing temperature on the Coefficient of performance (COP), compressor power and system heating capacity were evaluated. Results show that varying the condensing temperature an ideal point in which the system presents maximum performance can be determined. For R134a and R600a as refrigerants in low and high temperature cycles, the ideal operating point requires power of 3.04kW and 5.57kW, respectively, for a heating capacity of 11.58kW. From the environmental point of view, it was found that the proposed system reduces the GWP by 59.8% and 36.7% compared to wood and gas boiler systems combined with a refrigeration system.*

Keywords: *Heat pump, Steam generation, Industrial process*

1. INTRODUCTION

The Brazilian industrial sector is responsible for consuming 32% of the energy produced in the country, in which about 80% corresponds to thermal energy (EPE, 2022). About this energy demand, approximately 18.2% are applied to generate process heat at low temperature (<150ºC) (Solar Payback, 2018), In the year of 2021 it was responsible for the consumption of 12.2 Mtoe (EPE, 2022). In order to meet this heat demand, industries employ saturated water vapor as working fluid.

The steam production process in the industrial sector is typically obtained through the use of wood boilers or Liquefied Petroleum Gas (LPG). Such devices, even if they meet the thermal load of the processes, are responsible for generating significant amounts of waste heat in the industrial network, whose waste contributes to the increase in operating costs and the emission of particles and greenhouse gases. Thus, the high financial and environmental cost tied to the supply of thermal energy in industrial processes, established a favorable environment for the development of studies in order to promote the increase in the energy efficiency of equipment and systems in order to maximize the use of its resources.

Heat pumps (HP) are electromechanical equipment that aims to transfer heat, using an external power, from a cold source to a hot source (Bergman, 2011). Such devices can be applied in both heating and cooling processes, which operate according to thermodynamic absorption cycles or by mechanical vapor compression, the last being the most widespread.

Mechanical steam compression pumps are composed of interdependent subsystems such as evaporator, compressor, condenser and expansion valve. The process of transferring thermal energy in these devices occurs mechanically through the useful work performed by the compressor, whose drive depends on an external power source (usually of an electrical nature). This energy is transferred between the components through the circulation of a refrigerant. The direction of heat flow in these systems is from the evaporation temperature, which is the lowest temperature in the cycle, to the highest temperature, that of condensation.

Although they are very efficient (Schlossera et al., 2019), given that when the thermal load is established, the mechanical energy supply represents only a fraction of the energy load generated, still present a limitation in the operational performance in meeting the demand for high temperatures when they operate in a single stage. In this case, HP can reach temperatures of 90°C, and in some cases about 160°C when aided by some pre-commercial technologies in combination with some high-performance refrigerants with low global warming potential (Arpagaus et al., 2018) (Akmese et al., 2021) (Jiang et al., 2022).

Among these auxiliary technologies for cogeneration of thermal energy, double-cascade heat pumps (DCHP), in recent years, have become a promising application technology, since they can increase the efficiency of operation when compared with a single-stage heat pump, since they are composed of two cycles of steam compression, that interact through an intermediate heat exchanger located between the low power cycle evaporator and the high power cycle condenser (Li et al., 2019) (Li et al., 2018) (Song et al., 2017) (Cox et al., 2022). The different compression rates in each cycle are what makes it possible to reach high temperature values and can be applied to provide vapor to atmospheric pressure.

Although these innovations are very promising, they are little widespread in Brazil. The lack of knowledge about this technology and the low-price competitiveness between electricity and conventional fuels for process heat generation are some of the barriers that persist to the broad adoption of DCHP. Thus, the identification of industrial applications that demonstrate an opportunity to improve operational performance related to the reduction of process costs and that generate less impact to the environment, becomes a favorable option for the implementation of these pumps.

Thus, for an industry to become more competitive in the market, it associates strategies to improve environmental management with the application and development of technological innovations that minimize energy waste, optimizing its productive and strategic chain, making it more functional. Therefore, this work aims to analyze the technical and environmental feasibility of the use of double cascade heat pumps (DCHP) to perform steam generation.

2. METHODOLOGY

The project presented here describes the thermal modeling of a DCHP system in an industrial process to meet the demands of atmospheric pressure vapor generation (T= 100ºC) and cooling of 0.4m³/h water from ambient temperature to 6ºC.

The proposed system was dimensioned from the energy balance of each component of DCHP using the laws of thermodynamics. DCHP modeling was performed in Python in conjunction with the CoolProp® tool, which provides the thermophysical properties of water and coolants. From the process demands, refrigerants that had the capacity to operate under subcritical conditions were selected, i.e., below their temperature and critical pressure points. Thus, the optimum operating condition of the system, given by the maximum value of the Coefficient of Performance (COP), was obtained by adjusting the operating conditions of the intermediate exchanger. This optimization process is carried out considering various condensing temperatures.

The environmental impact analysis was performed from the comparative analysis of the equivalent carbon footprint between DCHP and boilers using different fuels for steam generation in conjunction with refrigeration systems to meet the cooling demand.

2.1 Description of DCHP

The proposed system to meet the heating and cooling demands consists of two cycles of steam compression, which operate separately at low and high temperature (Bansal and Jain, 2007). The Schematic diagram of the DCHP is shown in Fig. 1 and the diagrams representing the thermodynamic cycles are shown in Fig. 2.

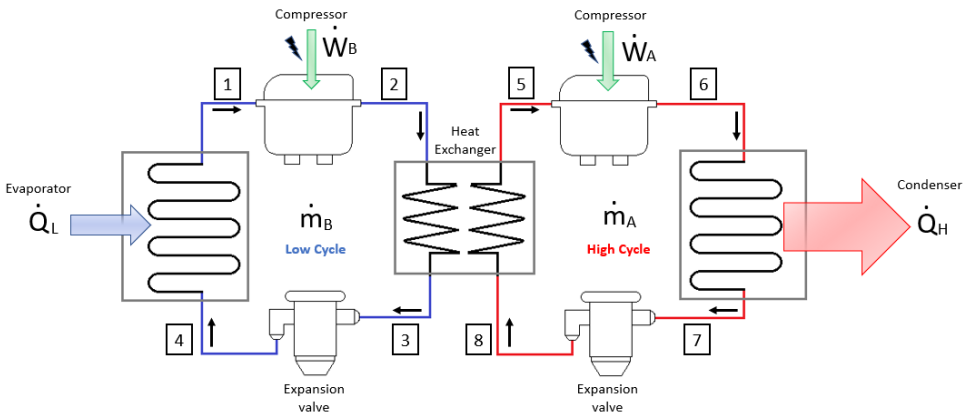

Figure 1. Double cascade heat pump system diagram.

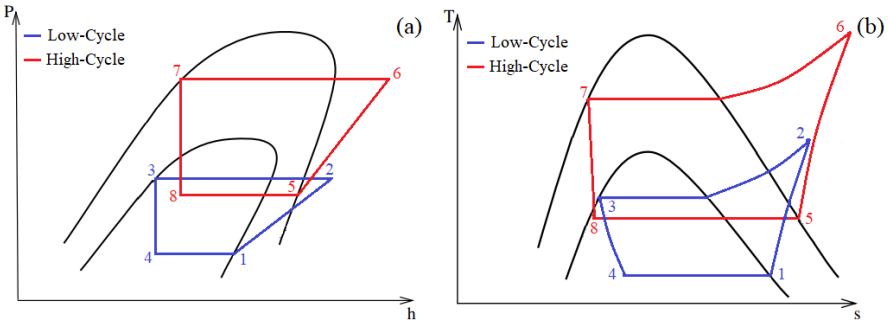

Figure 2. Pressure-Enthalpy P-h (a) and Temperature-Entropy T-s (b) diagram for a DCHP.

The heat removed by the evaporator in the low-temperature cycle (4-1) comes from the demand for cooling of cold water. In the low temperature stage, the refrigerant absorbs heat in the evaporator (4-1), which is the lowest temperature region of the system, becoming saturated steam (1). It is through the evaporator that the thermal exchange required to meet the cooling demand of the industrial process takes place. The refrigerant vapor coming out of the evaporator is then adiabatically compressed into the compressor (1-2), becoming overheated steam (2). This high pressure and temperature steam that comes from the compressor enters the intermediate heat exchanger (2-3) and transfers energy to the high-power cycle, transforming its physical state into saturated liquid at high pressure and temperature (3). Then the coolant enters the expansion valve, which is responsible for lowering the pressure of the coolant through an isenthalpic expansion process (3-4). This process is responsible for promoting the return of the fluid at the lowest pressure and temperature within the cycle, to the evaporator (4). The return of the fluid to the evaporator (4-1) determines the end of the refrigerant cycle in the low temperature stage.

In the high temperature stage, the refrigerant absorbs the thermal energy released by the low-power cycle in the intermediate heat exchanger (5-8), becoming saturated steam (5). The refrigerant vapor is adiabatically compressed in the high-power compressor (5-6), making it overheated steam (6). This high pressure and temperature vapor enters the condenser transforming its physical state into saturated liquid at high pressure and temperature (7), due to the transfer of energy to water (6-7), which is used to generate steam. Then the coolant enters the expansion valve (7-8), lowering the pressure of the coolant. Thus, the refrigerant returns to the intermediate heat exchanger (8) with the lowest pressure and temperature within the cycle. The return of the fluid to the heat exchanger (8-5) determines the end of the refrigerant cycle in the high temperature stage.

2.2 System modeling

Thermodynamic modeling was performed in order to evaluate the performance of DCHP. The model considers the components of the two cycles (high and low): evaporator, compressors, intermediate heat exchanger, condenser and expansion valves. Some hypotheses were adopted to characterize the model:

(1) Steady state operation, so the properties of refrigerants are invariable at each point of analysis over time.
(2) Compressors operate adiabatically.
(3) Refrigerants are saturated at the outlet of the evaporator, intermediate heat exchanger and condenser.
(4) Expansion valves perform an isenthalpic strangulation process.
(5) The effects of kinetic energies and potential of refrigerants are negligible.
(6) Heat losses and pressure losses in pipes, evaporator, intermediate heat exchanger and condenser are not considered.

According to the hypotheses mentioned above, thermal analysis was performed using the first law of thermodynamics and the principle of mass conservation. The first law is defined by the principle of energy conservation (Moran et al., 2013). The energy conservation equation for an open system is given by:

$$\dot{Q} - \dot{W} + \sum_{in} \dot{m} \cdot h - \sum_{out} \dot{m} \cdot h = 0 \quad (1)$$

where $\dot{Q}$ is the amount of total amount of heat transferred (kW), $\dot{W}$ is the amount of useful work received by the system (kW), $\dot{m}$ is the mass flow of coolant circulating within the cycle (kg/s) and h is the specific enthalpy of the refrigerant (kJ/kg).

2.2.1 Evaporator

For a flow of 0.4 m³/h of water, the cooling demand establishes the change of its temperature from 20°C to 6°C (6.5 kW). This water passes through a heat exchanger with an estimated efficiency of 75%. Thus, the heat transferred to the

refrigerant at the evaporator is 4.9 kW (6.5 kW x 0.75), equivalent to 4,213.2 kCal/h. Thus, the heat at the entry of BCDC into the evaporator is given by the mass flow and the difference of enthalpy between points 1 and 4, as follows:

$$\dot{Q}_L = \dot{m}_B \cdot (h_1 - h_4) \tag{2}$$

The specific enthalpy value of point 1, as illustrated in the diagram of Fig. 1, was first determined a priori from the fluid temperature (0°C) in the saturated vapor condition. The value of the specific enthalpy of point 4 was determined based on the value of the enthalpy of the fluid inlet in the expansion valve (saturated liquid at the condensing temperature of the intermediate exchanger), since the process is isenthalpic (h4 = h3).

Thus, knowing the value of the amount of heat to be removed by the evaporator (1-4) and the respective values of enthalpy input and output of the refrigerant, it is possible to determine the value of the mass flow of the refrigerant in the low-cycle:

$$\dot{m}_B = \frac{\dot{Q}_L}{(h_1 - h_4)} \tag{3}$$

2.2.2 Low and high cycle compressor

The theoretical power of the compressor is determined according to the evaporation temperature and the condensing pressure of the refrigerant (Moran et al., 2013). The compressor is driven by an electric motor. In this way, the compressor power at the low and high cycle can be defined as:

$$\dot{W}_B = \frac{\dot{m}_B \cdot (h_{2s} - h_1)}{\eta_{sB} \cdot \eta_v \cdot \eta_e} \tag{4}$$

$$\dot{W}_A = \frac{\dot{m}_A \cdot (h_{6s} - h_5)}{\eta_{sA} \cdot \eta_v \cdot \eta_e} \tag{5}$$

where $\dot{m}_B$ and $\dot{m}_A$ are the mass flows of refrigerants at low and high temperature cycles, η_{sB} is the isentropic efficiency in the low cycle: $\eta_{sB} = (h_{2s} - h_1)/(h_2 - h_1)$, η_{sA} is the isentropic efficiency in the high cycle: $\eta_{sA} = (h_{6s} - h_5)/(h_6 - h_5)$, η_v is the volumetric efficiency of the compressor (%) and η_e it is the efficiency of the electric motor (%). In this analysis, η_v = 80% (Ma et al., 2018) and η_e = 96% (Procel Info, 2017).

To determine the temperature of point 2, it was initially considered that the compressor operates according to an isentropic process ($S_{2s} = S_1$), in order to obtain the temperature limit value at this point (T_{2s}). Thus, maintaining the pressure ($P_{2s} = P_2$), it is observed that a higher temperature is ($T_2 > T_{2s}$) making the fluid in superheated steam.

Hence, in order to obtain this value, in addition to considering the conservation of the mass ($\dot{m}_1 = \dot{m}_2$), it was necessary to determine the coefficient of adiabatic expansion ($\gamma = Cp/Cv$) and considering that the compression process is adiabatic and reversible we have for points 1 and 2:

$$P_1 \cdot V_1^{\gamma} = P_2 \cdot V_2^{\gamma} \tag{6}$$

In view of this equation, a relationship between the pressures and fluid densities can be established at points 1 and 2, obtaining the value of the fluid density at point 2 (ρ_2). In this way, you can determine the temperature value of point 2 depending on its density and pressure. Thus, the specific enthalpy value at point 2 was determined as a function of pressure (P_2) and temperature (T_2).

The specific enthalpy value of point 6 was determined following the same thermodynamic procedure as point 2, however, the compressor discharge pressure value of the high cycle (P_6) and the fluid output temperature in this compressor (T_6) was considered.

2.2.3 Intermediate heat exchanger

For the low power cycle, the condenser is the intermediate heat exchanger with heat flow given by:

$$\dot{Q}_T = \dot{m}_B \cdot (h_2 - h_3) \tag{7}$$

The specific enthalpy value of point 3 was determined based on the discharge pressure value of the cycle compressor ($P_3 = P_2$) and the saturated liquid state. For the high-power cycle, this intermediate exchanger is your evaporator. The energy balance in the intermediate exchanger is given by:

$$\dot{m}_B \cdot (h_2 - h_3) = \dot{m}_A \cdot (h_5 - h_8) \tag{8}$$

The specific enthalpy value of point 5 (saturated steam) was determined from the condensing temperature value of the low-added cycle of ΔT=5°C, aiming at the low consumption of electricity by compressors (Bansal and Jain, 2007). At this point the pressure P_5 is known. In view of that P_5=P_8, and what a specific enthalpy value at this point is the value of the fluid inlet enthalpy in the expansion valve (saturated liquid at the temperature of the condenser of the high cycle), since the process is isenthalpic ($h_7 = h_8$).

So, knowing the values of the enthalpy of the refrigerants, as well as the value of the mass flow of the low-cycle refrigerant, it is possible to determine the mass flow of the refrigerant in the high cycle:

$$\dot{m}_A = \frac{\dot{m}_B \cdot (h_2 - h_3)}{(h_5 - h_8)} \tag{9}$$

2.2.4 Low and high cycle expansion valve

In the process of throttling of refrigerants there is a reduction of pressure, which represents a loss of load to the system. However, considering that there is no heat transfer or work under the system, it can be observed that there is an increase in the flow rate of the fluids. Since mass flows remain constant in cycles, there is a change in their specific volumes. This change directly reflects on the variation of the internal energy of the fluids and, therefore, their temperatures also vary. Thus, if we consider that the specific volume increases as the pressure decreases, the enthalpy difference must be null (isenthalpic process) to satisfies the first law of thermodynamics. Therefore, the physical state of the refrigerant at points 4 and 8 represent a biphasic mixture (liquid + steam) (Moran et al., 2013).

2.2.5 Condenser

The transfer of DCHP to the water storage tank is defined by:

$$\dot{Q}_H = \dot{m}_A \cdot (h_6 - h_7) \tag{10}$$

Where the specific enthalpy value of point 7 was determined based on the discharge pressure value of the cycle compressor ($P_7 = P_6$) and the saturated liquid state. The amount of heat received by water should be sufficient to change its physical state from saturated liquid, at ambient temperature, to saturated steam. This energy can be determined from a composition of sensitive heat and latent heat of water vaporization:

$$\dot{Q}_H = \frac{\dot{v}_{water} \cdot \rho_{water}}{3600} \cdot (Cp_{water} \cdot \Delta T_{water} - L_v) \tag{11}$$

where $\dot{v}_{water}$ is the volumetric flow of saturated water vapor (m³/h), ρ_{water} is water density (kg/m³), Cp_{water} is water-specific heat constant pressure (kJ/kg.K), ΔT_{water} is the difference in water temperature between ambient temperature and vapor temperature saturated at atmospheric pressure (100 ºC) and L_v is the latent heat of water vaporization (kJ/kg).

2.3 Selection of refrigerants fluids

The selection of refrigerants was performed considering high critical operating temperatures, for example, higher than 100 °C and low pressures at operating temperatures. As a reference, Fig. 3 presents a diagram of the relationship between pressure and evaporation temperature for different types of refrigerants most commercially used in heat pumps (Industrial Heat Pumps, 2022).

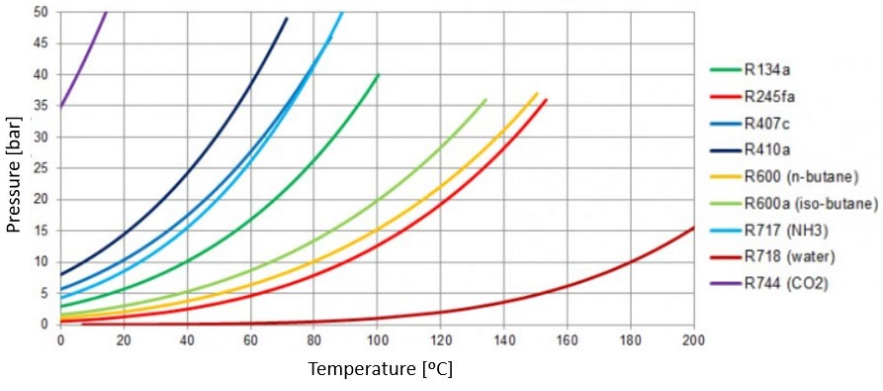

Figure 3. Evaporation Pressure-Temperature Diagram.
Available from: https://bit.ly/3msmQku

For the low cycle, an evaporation temperature of T_1 = 0ºC was considered, since the heat flow should occur in the direction of the medium for the heat pump during the entire water-cooling process. The condensing temperature of this cycle was defined by the maximum values of temperature and discharge pressure in the low-cycle compressor and the same values related to the suction of the high-cycle compressor.

For the high-cycle, aiming to achieve a low consumption of electric power by the compressors, the evaporation temperature was determined considering a temperature difference (ΔT) of 5ºC related to the condensing temperature of the low cycle refrigerant (Bansal and Jain, 2007). The condensing temperature of this cycle was determined based on the minimum temperature of T_7 = 100ºC, whose value is fundamental to establish the direction of the heat flow from the pump to the water storage tank during the entire steam generation process.

Therefore, the R600a refrigerant (isobutane) was chosen to make up the high-cycle, since it has a critical temperature above 100°C and belongs to the family of organic refrigerants (composed of hydrocarbons). These fluids have low Ozone Depletion Potential (ODP) and low Global Warming Potential (GWP), not contributing to the greenhouse effect. The selection of this fluid sought to meet the Kigali Amendment of the Montreal Protocol, whose main objective is to establish the gradual replacement of artificial refrigerants (hydrofluorocarbons - HFCs) in thermal systems (IDEC, 2022).

For the low-cycle, the R134a was chosen, in view of which has a critical temperature above 100°C and is the most widespread on the market (Pavel Makhnatch, 2014). Table 1 presents the thermophysical properties of the chosen refrigerants (Gas Servei, 2022) (Embraco, 2020).

Table 1. Thermophysical properties of R134a and R600a.

Refrigerant	Critical temperature (ºC)	Critical pressure (bar)	ODP (100 years)	GWP (100 years)
R134a	101,1	40,6	0	1430
R600a	134,6	36,4	0	4

*ODP: Measures the ozone depletion potential, ranging from 0 to 1, so if the ODP is close to zero, the impact on the ozone layer is small.
*GWP: Measures the effect of warming produced by gases in the atmosphere over time in relation to amounts of CO_2 (by weight).

2.4 Cascade system performance

The DCHP system cooling COP is defined as the relationship between the heat absorbed by the evaporator and the total work performed by the compressors:

$$COP_C = \frac{\dot{Q}_L}{\dot{W}_B + \dot{W}_A} \tag{12}$$

The cascade system heating COP is defined as the relationship between the heat released by the condenser and the total work performed by the compressors:

$$COP_H = \frac{\dot{Q}_H}{\dot{W}_B + \dot{W}_A} \tag{13}$$

3. GLOBAL WARMING POTENTIAL ASSESSMENT

The analysis of environmental impacts related to a steam generation process for industrial use resulting from the replacement of conventional equipment present in the sector for the system proposed in this study, a comparative approach was performed using the life cycle evaluation method (LCA). This study is indicated to evaluate the impacts related to all stages, from the extraction of the raw material to the consumption or reuse of a resource linked to a process or product (ABNT ISO/NBR 14040-14044, 2009).

For the purposes of the analysis present in this study, the Ecoinvent v.3.8® database was used, whose chosen model was the "*Allocation at the point of substitution (APOS)*". The method of analysis selected was the *ReCiPe 2016 Hierarchist* (Huijbregts et al., 2017). For this study, it was only chosen to evaluate only the impact of global warming potential (GWP), given in kg of $CO_{2(eq)}$/kWh.

The impact of the use of DCHP in meeting the thermal demands of cooling and heating is determined by comparing the GWPs for the conventional system (boilers activated with LPG and firewood, and the cooling system) and the system using the DCHP. The GWP for each process was obtained from the multiplication between the consumption of thermal or electric energy (in kWh) and the impact factor obtained from the database. In relation to the refrigerants used in DCHP and the refrigeration system, the value of the amount of $CO_{2(eq)}$ obtained by multiplying the mass of the fluid in kg by the specific GWP of the fluid was increased.

4. RESULTS

This section presents the performance of the DCHP system using the refrigerants R134a and R600a for the low and high temperature cycles, respectively. The DCHP system was analyzed under optimized COP conditions under different condenser temperatures. In addition, at the end of this section, the environmental impact related to global warming potential for this cascading system compared to conventional steam generation methods was evaluated.

4.1 Cascade system performance analysis

The first stage of thermodynamic analysis for certain DCHP working conditions was performed to obtain the best combination of operation in the cycles. Thus, computational simulations were performed varying the average temperature of the intermediate heat exchanger (T_m) in order to obtain the condensation temperature of the low cycle and evaporation of the high cycle that returned the maximum COP value. The interval of temperature variation of the intermediate exchanger was from 10ºC to 90ºC, in order to meet the conditions of subcritical operation of the fluids during all simulations. The results of the analyses are shown in Fig. 4.

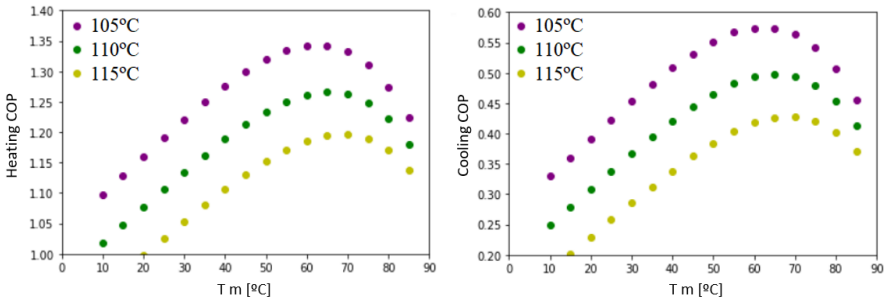

Figure 4. COP diagram as a function of the temperature of the intermediate heat exchanger considering various temperatures at the condenser outlet in the range of 105ºC to 115ºC.

For example, considering the condensing temperature (T_{cond}) in the high cycle (point 7) of 105ºC (P_{sat} = 21.78 bar), it was observed that the highest value of heating COP, approximately 1.34, it is obtained for an average temperature of the heat exchanger of 61ºC. Thus, the condensing temperature of the low cycle (T_3) was 63ºC (P_3 = 18.25 bar) and the evaporation temperature of the high cycle (T_5) obtained was 58ºC (P_5 = 8.39 bar) (Bansal and Jain, 2007). The thermodynamic properties of the fluids considered in this analysis are presented in the Tab. 2, and the T-s (temperature-entropy) and P-h (pressure-enthalpy) diagrams are shown in Fig. 5.

Table 2. Description of thermodynamic properties for T_m = 61ºC.

Points	Pressure [bar]	Temperature [ºC]	Enthalpy [kJ/kg]	Entropy [kJ/kg.K]
1	2.9	0.0	398.6	1.72
2	18.2	79.3	448.4	1.76
3	18.2	63.4	293.2	1.30
4	2.9	0.0	293.2	1.34
5	8.4	58.4	631.6	2.33
6	21.7	118.1	719.1	2.47
7	21.7	105.0	482.3	1.85
8	8.4	58.4	482.3	1.88

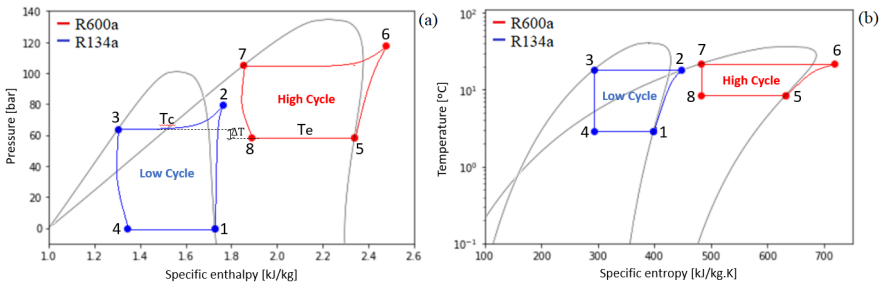

Figure 5. Diagrams T-s (a) and P-h (b) for T_m = 61ºC.

Figure 4 shows the dependence of high-cycle COP and low-cycle COP as a function of the temperature of the intermediate heat exchanger is shown in Fig. 6.

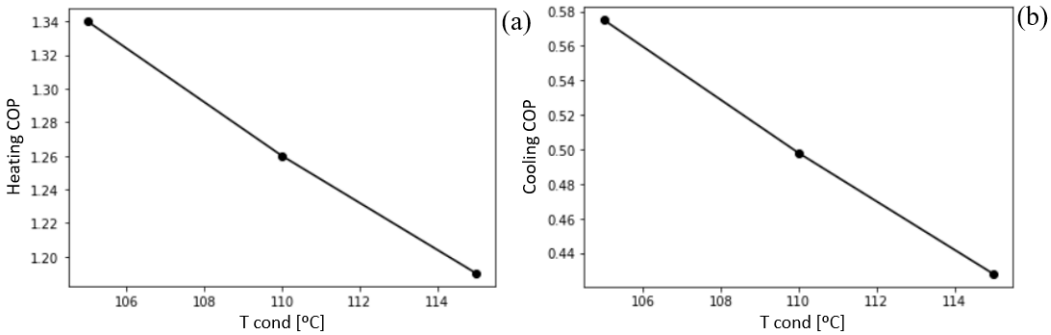

Figure 6. Dependence of heating COP (a) and cooling COP (b) as a function of condenser outlet temperature.

Under the conditions where the COP was maximum, the compressor power, mass flows and isentropic efficiencies were determined in the high and low temperature cycles, as well as the heating capacity of DCHP. The results of these analyses are shown in Fig. 7.

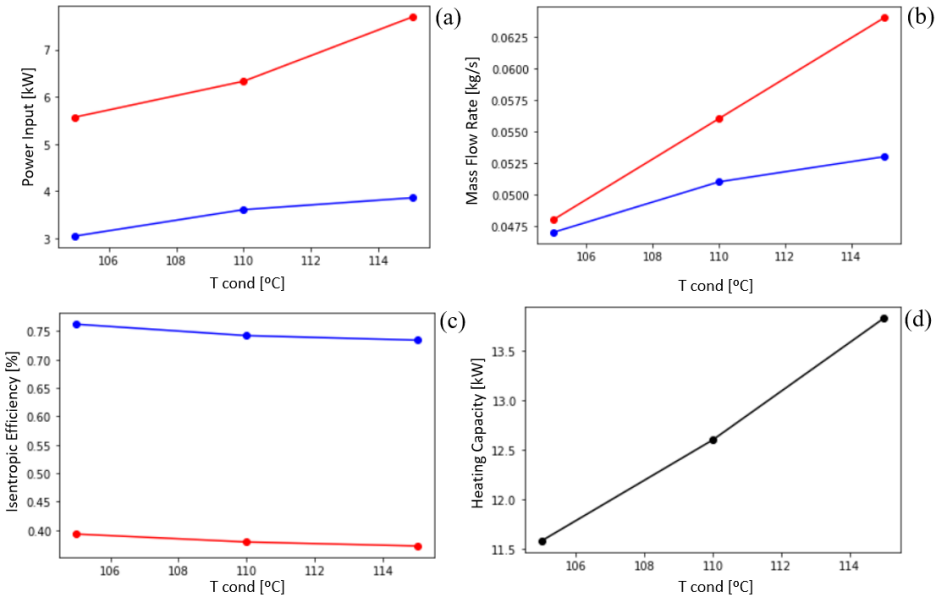

Figure 7. Diagrams of input power (a), mass flows (b), isentropic efficiencies (c) and heating capacity (d) as a function of temperature at condenser outlet.

Therefore, it was observed that the COP decreases as the condensing temperature of the high cycle increases. This fact is due to the variation in the input power of the compressors in each cycle, as a consequence of the variation of the mass flows of refrigerants, and the heating capacity. Thus, for T_{cond} = 106°C, the input powers of the compressors for the maximum COP were 3.04 kW (η_s = 76.2%) and 5.57 kW (η_s = 39.3%) for the cycles of low and high temperatures, respectively. The mass flows required to meet the process demands were 0.047 kg/s and 0.049 kg/s for low and high temperature cycles, generating a heating capacity ($\dot{Q}_H$) of 11.58 kW, providing steam to a volumetric flow of 0.015 m³/h.

4.2 Cascade system environmental analysis

The environmental impact related to the global warming potential for each system is found in the Tab. 3. For calculation purposes, a mass of 1 kg was estimated for refrigerants R134a and R600a to make up DCHP. For the conventional refrigeration system, R134a was considered as refrigerant and a power supply of 1.5 kW for compressor activation. This power value was estimated by typical commercial values of condensing units that meet the cooling capacity required for the supply of cold water (4,124.2 kCal/h).

The annual consumption values of conventional systems were estimated based on the Lower Calorific Value (LCV) of fuels (LCV_{LPG} = 11025 kCal/kg; LCV_{wood} = 2400 kCal/kg) (Alfa Laval Aalborg, 2022), at the typical efficiency values of the boilers (η_{LPG} = 30%; η_{wood} = 70%) (Jugjai and Rungsimuntuchart, 2002) (Chandrasekaran, 2011), in the amount of fuel consumed to meet the demands in the industrial sector analyzed (M_{LPG} = 4.5 kg; M_{wood} = 10 kg) and the duration of the processes per operation per day (heating: 1.5 h; cooling: 40 min) in one year. On the other hand, the consumption value of DCHP was defined based on the sum of the values of the compressor input powers in each cycle (3.04 kW + 5.57 kW) considering the 2 h operating time.

Table 3. Global warming potential in the current operation of the conventional system and using the heat pump.

Item	Description	Consumption kWh	CF	Total kg $CO_{2(eq)}$
1	Wood boiler	10690.1	0.531	5676.4
2	Gas boiler	9470.7	0.314	3066.9
3	Refrigeration system	252.0	0.230	1487.9
4	DCHP	6285.3	0.230	2879.6

(1)CF: Carbon footprint (kg $CO_{2(eq)}$/kWh)

Therefore, it can be evaluated that the implementation of DCHP to meet the demands of heating and cooling contributes effectively to the reduction of about 1675.2 kg $CO_{2(eq)}$ per year (decrease of 36.7%) in relation to the conventional refrigeration system and the gas boiler, and about 4284.7 kg $CO_{2(eq)}$ per year (decrease of 59.8%) in relation to the conventional refrigeration system and the wood boiler.

5. CONCLUSION

To meet steam generation and cooling demands typical of an industrial process, DCHP simulations operating with pair R134a and R600a showed that such demands can be met, since temperatures in the condenser above 100°C and evaporator temperatures of 0°C were reached. Additionally, DCHP had the lowest environmental impact since their CF was lower compared to the other technologies studied (wood and gas boilers along with the refrigeration system). Thus, the study of DCHP is an alternative to minimize energy and environmental costs within industrial processes of steam and cold-water generation.

6. ACKNOWLEDGMENTS

The authors would like to thank the support received by the Coordenação de Aperfeiçoamento de Pessoal de Nível Superior (CAPES), the Universidade de Pernambuco/Escola Politécnica de Pernambuco (UPE/POLI), the Universidade Federal de Pernambuco (UFPE) and the Instituto de Tecnologia de Pernambuco (ITEP).

7. REFERENCES

ABNT NBR ISO 14044:2009, Versão Corrigida 2014 – Gestão ambiental, Avaliação do Ciclo de Vida, Requisitos e orientações – Publicada em 21.07.2014.

Akmese, S., Omeroglu, G., and Comakli, O., 2021. “Photovoltaic thermal (PV/T) system assisted heat pump utilization for milk pasteurization”. *Solar Energy*, Vol. 218, pp. 35-47.

Alfa Laval Aalborg, 2022. “Poder Calorífico Inferior”. <https://bit.ly/3zKrL8 >.

Arpagaus, C., Bless, F., Uhlmann, M., Schiffmann, J., and Bertsch, S. S., 2018. “High temperature heat pumps: Market overview, state of the art, research status, refrigerants, and application potentials”. *Energy*, Vol. 152, pp. 985-1010.

Bergman, T. L., Incropera, F. P., Dewitt, D. P., and Lavine, A. S., 2011. *Fundamentals of heat and mass transfer*. John Wiley & Sons, New Jersey, 6th edition.

Bansal, P. K., Jain, S., 2007. “Cascade systems: past, present, and future”. *ASHRAE Transactions*, Vol. 113, pp. 245.

Chandrasekaran, S. R., Laing, J. R., Holsen, T. M., Raja, S., and Hopke, P. K., 2011. “Emission characterization and efficiency measurements of high-efficiency wood boilers. *Energy & fuels*, Vol. 25, n. 11, pp. 5015-5021.

Cox, J., Belding, S., and Lowder, T., 2022. “Application of a novel heat pump model for estimating economic viability and barriers of heat pumps in dairy applications in the United States”. *Applied Energy*, Vol. 310, pp. 118499.

EPE, 2022. “Plano Decenal de Expansão de Energia (PDE) 2031”. 11 Apr. 2022. <https://bit.ly/3E2x6rG>.

Gas Servei, 2022. “Dados Técnicos - R134a”. <https://bit.ly/3xoItr4>.

Embraco, 2020. “Guide for the use of HCs refrigerants R600a and R290”. <https://bit.ly/3aSJzUg>.

Huijbregts, M. A., Steinmann, Z. J., Elshout, P. M., Stam, G., Verones, F., Vieira, M., Zijp, M., Hollander, A., Van Zelm, R., 2017. “ReCiPe2016: a harmonized life cycle impact assessment method at midpoint and endpoint level”. *The International Journal of Life Cycle Assessment*, Vol. 22, n. 2, pp. 138-147.

IDEC, 2022. “Emenda de Kigali: benefícios de sua ratificação pelo Congresso Nacional”. <https://bit.ly/3n17mUO>

Industrial Heat Pumps, 2022. “Operating principles: Refrigerants”. <https://bit.ly/3msmQku>

Jiang, J., Hu, B., Wang, R. Z., Deng, N., Cao, F., and Wang, C. C., 2022. “A review and perspective on industry high-temperature heat pumps”. *Renewable and Sustainable Energy Reviews*, Vol. 161, pp. 112106.

Jugjai, S., Rungsimuntuchart N., 2002. “High efficiency heat-recirculating domestic gas burners”. *Experimental thermal and Fluid Science*, Vol. 26, n. 5, pp. 581-592.

Li, F., Chang, Z., Li, X., and Tian, Q., 2018. “Energy and exergy analyses of a solar-driven ejector-cascade heat pump cycle”. *Energy*, Vol. 165, pp. 419-431.

Li, X., Zhang, Y., Ma, X., Deng, N., Jin, Z., Yu, X., and Li, W., 2019. “Performance analysis of high-temperature water source cascade heat pump using BY3B/BY6 as refrigerants”. *Applied Thermal Engineering*, Vol. 159, pp. 113895.

Ma, X., Zhang, Y., Fang, L., Yu, X., Li, X., Sheng, Y., and Zhang, Y., 2018. “Performance analysis of a cascade high temperature heat pump using R245fa and BY-3 as working fluid”. *Applied Thermal Engineering*, Vol. 140, pp. 466-475.

Moran, M. J., Shapiro, H. N., Boettner, D. D., and Bailey, M. B., 2013. *Princípios de termodinâmica para engenheiros*. LTC, 7a edição.

Pavel Makhnatch, 2014. “Low GWP refrigerants for high temperature heat pumps”. 21 Sep. 2014. <https://bit.ly/3O7wvIW>.

Procel Info, 2017. “Troca de motores como indutora de competitividade na indústria brasileira”. <https://bit.ly/3A2YfuP>

Schlossera, F., Arpagaus, C., and Walmsley, T. G., 2019. “Heat pump integration by Pinch analysis for industrial applications: a review”. *Chem. Eng. Trans*, Vol. 76.

Solar Payback, 2018. “Energia Termossolar para a Indústria: Brasil”. May. 2018. <https://bit.ly/3xnsuL3>.

Song, Y., Li, D., Cao, F., and Wang, X., 2017. “Theoretical investigation on the combined and cascade CO2/R134a heat pump systems for space heating”. *Applied Thermal Engineering*, Vol. 124, pp. 1457-1470.

8. RESPONSIBILITY NOTICE

The author(s) is (are) the only responsible for the printed material included in this paper.